



OPEN

# Common features in spatial livestock disease transmission parameters

Gert Jan Boender<sup>✉</sup> & Thomas J. Hagenaars

The risk of epidemic spread of diseases in livestock poses a threat to animal and often also human health. Important for the assessment of the effect of control measures is a statistical model quantification of between-farm transmission during epidemics. In particular, quantification of the between-farm transmission kernel has proven its importance for a range of different diseases in livestock. In this paper we explore if a comparison of the different transmission kernels yields further insight. Our comparison identifies common features that connect across the different pathogen-host combinations analyzed. We conjecture that these features are universal and thereby provide generic insights. Comparison of the shape of the spatial transmission kernel suggests that, in absence of animal movement bans, the distance dependence of transmission has a universal shape analogous to Lévy-walk model descriptions of human movement patterns. Also, our analysis suggests that interventions such as movement bans and zoning, through their impact on these movement patterns, change the shape of the kernel in a universal fashion. We discuss how the generic insights suggested can be of practical use for assessing risks of spread and optimizing control measures, in particular when outbreak data is scarce.

Epidemics of highly contagious diseases in livestock such as Foot and-Mouth Disease (FMD) and high pathogenic avian influenza (HPAI) can have tremendous socio-economic consequences as well as devastating effects on animal health<sup>1,2</sup>. For developing effective contingency planning for the control of such epidemics, it is essential to use the data from previous epidemics to gain as much insight as possible in the quantitative characteristics of transmission, in particular of between-farm transmission<sup>3</sup>. These characteristics may include the observed effect of control measures such as animal movement standstill or zoning<sup>4</sup>. By means of using mathematical models fitted to describe these characteristics, past or current outbreaks in a given country are often being used to make extrapolations to current or future transmission risks in that same country<sup>5,6</sup>. For countries with no earlier or no informative outbreak, one may resort to extrapolation from epidemic patterns observed in other countries, addressing uncertainties about model representativity for the country of interest e.g. by exploring the sensitivity of the model outcomes to possible differences in parameter values<sup>7</sup>. For emerging diseases for which there is no previous epidemic that can be analyzed, what can we learn from the patterns observed in epidemic data of other livestock diseases? Here we present a general framework for the spatial transmission of livestock diseases that can help to underpin model extrapolations between control strategies, between countries, and also between diseases. It is built on the comparison of epidemic transmission risk patterns across a range of livestock diseases.

Our framework uses the transmission kernel as a central element in the modelling approach. Transmission kernels describe the distance-dependent probability of transmission from an infected to a susceptible farm, and have been used to describe the between farm transmission of different animal diseases<sup>5,6</sup>. Use of a transmission kernel avoids the modelling of specific transmission pathways where these are poorly known, and allows both the construction of risk maps as well as model simulation studies of the effectiveness of control measures<sup>5,6,8,9</sup>. The transmission kernel also facilitates the comparison of the distance-dependent characteristics of transmission between epidemics, between diseases, and between phases in one and the same epidemic differing in applied control measures, in particular in the type of animal movement restrictions that were applied<sup>10–12</sup>.

For the interpretation of the comparative kernel analyses results we can build on a body of literature that uses spatial kernels to describe movement and dispersal patterns<sup>13,14</sup>. One of the elements from this literature is a distinction between thin-tailed (i.e. exponentially bounded) and fat-tailed (i.e. power-law) kernels<sup>15</sup>. Whereas thin-tailed kernels generate 'diffusive' dispersal patterns with constant-speed travelling waves, a fat-tailed kernel produces 'super-diffusive' behavior lacking a finite velocity and yielding a patchy dispersal pattern<sup>15–18</sup>. In the

Wageningen Bioveterinary Research, P.O. Box 65, 8200 AB Lelystad, The Netherlands. ✉email: gertjan.boender@wur.nl

description of animal movement, thin-tailed kernels are a signature for an underlying Brownian random walk and fat-tailed kernels for Lévy-walk patterns; based on this distinction several studies demonstrate Lévy-walk patterns for animal movement<sup>19–22</sup>. Also human mobility appears to follow a Lévy walk<sup>23,24</sup>, and this could be of relevance to between-farm disease transmission as transmission between farms is likely caused in part by humans moving between the farms and thereby acting as passive vectors.

An important subtlety described by the so-called ‘truncated’ Lévy-walk model is the phenomenon that the fat-tailed/power-law behaviour is truncated by an exponential decline setting in above a cut-off distance scale. This truncated version of the Lévy-walk model describes super-diffusive movement on a distance small compared to, and diffusive movement on a scale large compared to, the cut-off distance<sup>25</sup>. In the case of human mobility, such a cut-off distance scale may reflect the existence of an area within which most of the movements are confined, e.g. an urban area for the movements of commuters<sup>26</sup>. For human travel mobility patterns the power-law exponent in the truncated Lévy walk appears to have a universal value of about 1.6<sup>17,23</sup>.

The aim of this article is to yield insight into the similarities and differences between a range of spatial patterns of animal disease transmission by comparison of the corresponding transmission kernels. In particular, we seek to investigate to which extent the observed between-farm transmission patterns can be categorized and interpreted using insights from the study of movement and dispersal patterns. We will use one and the same kernel parametrisation throughout such that parameter values can be directly compared. In our previous kernel analyses of between-farm transmission we have mostly adopted a so-called Cauchy form (defined below) to parameterize the kernel, motivated in part by the fact that it was identified as having the lowest AIC amongst a set of alternatives studied in<sup>6</sup>, in which the Lévy-walk kernel was not included. Recent analyses suggest that the (non-truncated) Lévy-walk kernel produces an even better fit to spatial transmission data from certain livestock disease epidemics<sup>10,27</sup>.

Therefore we re-analyzed eight epidemic datasets available to us using the Lévy-walk kernel; basic characteristics of these eight datasets are listed in Table 1 and 2. In addition to this, we assembled from the literature three Lévy-walk kernels estimated for other animal disease epidemic datasets. Together, the 11 datasets comprise a broad set of different host–pathogen combinations, including viral and bacterial pathogens. The resulting set of

Nr	Disease	Year	Country	Strategy	Kernel model of existing analysis
1.	FMD <sup>10</sup>	Before 23rd February 2001	UK	NMNZ	Lévy Walk
2.	SVD <sup>12</sup>	2006	Italy	NMNZ	Reference
3.	Q fever <sup>28</sup>	2007–2010	The Netherlands	NMNZ	Reference
4.	BT <sup>11</sup>	2006	Belgium	NMZ	Reference
5.	BT <sup>11</sup>	2006	Germany	NMZ	Reference
6.	CSF <sup>29</sup>	1997–1998	Netherlands	M	Reference
7.	FMD <sup>10</sup>	Post 23rd February 2001	UK	M	Lévy Walk
8.	FMD <sup>8</sup>	2001	The Netherlands	M	Reference
9.	HPAI <sup>6</sup>	2003	The Netherlands	M	Reference
10.	SVD <sup>12</sup>	2007	Italy	M	Reference
11.	FMD <sup>27</sup>	2010	Japan	M	Lévy Walk

**Table 1.** List of 11 epidemic datasets analyzed, ordered by applied control strategy (in order of increasingly stringent measures: no movement ban nor zoning (NMNZ), no movement ban but zoning (NMZ), and a movement ban (M)) and year. Datasets 1 and 7 represent two time periods of one and the same epidemic; for brevity we often refer to all 11 datasets as ‘epidemics’ in the main text.

Nr	Disease	Disease type	Affected species	Population size	Number of outbreaks	Reference
2 <sup>12</sup>	SVD	viral	Pigs	7600	36	12,40
3 <sup>28</sup>	Q fever	bacterial zoonotic	Goats	404	176	28
4 <sup>11</sup>	BT	vector-borne viral	Cattle Sheep	239,336	1119	11,41,42
5 <sup>11</sup>	BT	vector-borne viral	Cattle Sheep	87,007	880	11,43
6 <sup>29</sup>	CSF	viral	Pigs	23,131	428	29
8 <sup>8</sup>	FMD	viral	Cattle Goats	94,506	26	8,44
9 <sup>6</sup>	HPAI	viral zoonotic	Poultry	5360	241	6
10 <sup>12</sup>	SVD	viral	Pigs	7600	17	12,40

**Table 2.** Basic characteristics of eight epidemics/epidemic datasets analyzed. For further details we refer the reader to the original publications on these datasets.

11 Lévy-walk kernels, each one determined by estimated values for four kernel parameters, allows us to compare the results to see if similarities extend across a broad set of livestock disease transmission patterns. Two of the four parameters are of highest importance in our analysis, as together these two largely determine the shape of the distance dependence. As a formal framework for the comparison between the 11 estimated kernels, we (1) apply a hierarchical clustering analysis to the set of 11 pairs of maximum-likelihood values for these two kernel shape parameters, and (2) correlate the clusters found to the type of control strategies applied during the 11 epidemics. A descriptive overview of the epidemics analyzed is given as part of the Materials and Methods. In the Results, the estimated Lévy-walk model parameters for each epidemic are presented, the hierarchical clustering analysis is carried out, and clusters found are correlated with applied control strategies. In the Discussion, we present the insights obtained and their practical relevance for assessing risks of spread and optimizing control measures, in particular when outbreak data is scarce.

## Material and methods

We assemble and compare the Lévy-walk kernel fits to 11 different between-farm transmission datasets. These datasets are listed in Table 1. Three of the datasets were already analyzed using Lévy-walk kernels in the literature, namely two parts of the UK 2001 FMD epidemics and the 2010 FMD epidemic in Japan<sup>10,27</sup>. The remaining eight datasets of livestock epidemics or parts of epidemics<sup>6,8,11,12,28,29</sup> are reanalyzed here by fitting truncated Lévy-walk kernels. These eight comprise the 2006 Q fever epidemics in the Netherlands, two parts of the Swine Vesicular Disease (SVD) epidemics in 2006/2007 in Italy, the 2001 FMD epidemic in the Netherlands, the 2003 HPAI epidemic in the Netherlands, the 1997/1998 Classical Swine Fever (CSF) epidemic in the Netherlands, and the 2006 Blue Tongue (BT) epidemics in Germany and Belgium. These eight epidemic datasets were previously analyzed individually using the ‘Cauchy’ form of the transmission kernel

$$\lambda(r) = \frac{\lambda_0}{1 + \left(\frac{r}{r_0}\right)^\alpha},$$

in which  $r$  is the Euclidean distance between an infectious and a susceptible farm,  $\lambda_0$  represents the amplitude of the transmission kernel and is interpreted as the transmission hazard for very small distance (‘distance zero’) between the infectious and the susceptible farm, and  $r_0$  is a characteristic distance, also referred to as ‘kernel offset’<sup>10</sup>. It is the distance where the transmission hazard has become half as large as at distance zero, and therefore it has an influence on the distance dependence of the kernel for distances up until a few times  $r_0$ . The parameter  $\alpha$  is a scaling exponent that determines how fast the long-distance transmission probability declines, and its influence on the kernel shape dominates over the influence of  $r_0$  for distances a few times larger than  $r_0$  and beyond. In more detail, the role of  $\alpha$  is that its value indicates whether transmission is short-ranged ( $\alpha > 3$ ), intermediate-ranged ( $2 < \alpha \leq 3$ ), or long-ranged ( $\alpha \leq 2$ )<sup>11</sup>. In this paper we keep the Cauchy kernel results for reference, to compare the fits to those using the Lévy-walk kernel. We use the following parametrization for the (truncated) Lévy-walk kernel<sup>23</sup>:

$$\lambda(r) = \frac{\lambda_0}{\left(1 + \frac{r}{r_0}\right)^\alpha} \exp\left(-\frac{r}{\kappa}\right),$$

in which the additional parameter  $\kappa$  is a cutoff distance truncating the Lévy-walk behavior to a finite spatial range. The parameter estimates are obtained Maximum Likelihood (ML) estimation, and confidence bounds using the likelihood-ratio test. As the kernel amplitude  $\lambda_0$  does not inform about the distance dependence of transmission, we only report its estimated values in the Supplementary Information for completeness. We note that the estimate for the cutoff distance  $\kappa$  is only informative if it is smaller than the ‘extent’ of the area spanned by the dataset; if larger, then no truncation is detected on the distance scales covered by the data. The likelihood that is maximized for the kernel estimation is constructed in the following way. For each farm an infection status (susceptible (S), becoming infected (C), latent (E), infectious (I), removed (R)) is assigned per time unit (day or week depending on dataset). Based on this, we obtain a set of possible infection events (a farm  $i$  with status I and a farm  $j$  with status C in the same time unit) and a set of escape events (a farm  $i$  with status I and a farm  $j$  with status S in the same time unit).  $\Lambda_j^C$  is the set of all farms  $i$  with status I at the start of the time unit in which farm  $j$  has status C.  $\Lambda_j^S$  is set of all farms  $i$  with status I for at least one time unit during which farm  $j$  has status S and  $N_{ij}^S$  is the number of time units for which  $i$  has status I and  $j$  has status S. As the escape probability during each one of such time units is given by  $\exp(-\lambda(r_{ij}))$ , where  $r_{ij}$  is the Euclidean distance between farm  $i$  and farm  $j$ , it is easily derived that the combination of all events has the following likelihood:

$$L(\lambda_0, \alpha, r_0, \kappa) = \prod_{j \in \Phi} \left( 1 - \prod_{i \in \Lambda_j^C} \exp(-\lambda(r_{ij})) \right) \prod_{k \in \Omega} \prod_{i \in \Lambda_k^S} \exp(-\lambda(r_{ik}) N_{ik}^S),$$

where  $\Phi$  is the set of all case farms except for the index case farm, and  $\Omega$  the set of all farms except for the index case farm.

The kernel is defined as a transmission hazard between two given individual farms, and its parameters are assumed to be homogeneous across the geographical area where the outbreaks occurred; in particular these parameters are assumed to be independent of farm density. To our knowledge there are no examples in the literature of epidemics in livestock where a regionally stratified kernel analysis produces significant differences in the

shape parameters of the transmission kernel; e.g.<sup>30</sup> noted that for FMD in 2001 in Great Britain ‘No significant regional [...] differences in the spatial transmission kernel were found, although statistical power was limited in areas outside Cumbria by lower case incidence’.

During the 11 epidemics the control strategy was either a movement ban (M), or no movement ban but zoning (NMZ), or no movement ban nor zoning (NMNZ). Zoning was applied in the 2006 BT epidemic in Germany with a typical zone radius of about 20 km and in the 2006 BT epidemic in Belgium, with spillover to the Netherlands and France, in which during the main part of the epidemics Belgium was considered to be one single zone corresponding approximately to a radius of about 140 km (half the extent of the country)<sup>11,31</sup>. Using the Akaike’s Information Criterion (AIC) the model fit of the Lévy-walk kernel was compared that of the reference (i.e. Cauchy) kernel (AIC<sub>0</sub>). Differences in AIC’s are considered to be significant if larger than 2<sup>32,33</sup>.

In order to objectively identify categories of epidemic transmission patterns we carried out a hierarchical clustering analysis using the estimated parameter pairs  $\{\alpha, \kappa\}$ <sup>34</sup>. Here we used a Euclidean distance function after rescaling both parameters to take values between 0 and 1. The rescaling was carried out using a logistic scaling function, in which for each of the two parameters the scaling factor was set to the median value across all 11 estimates. To assess the statistical significance of correlation between the clusters found and the type of control strategies applied during the 11 epidemics, we calculate a p-value by basic combinatorics.

## Results

The estimated parameters for the Lévy-walk kernel for the 11 epidemics are given in Table 3; for plots of the 11 kernel shapes we refer to Fig. S1. Amongst the eight epidemics we re-analyzed here, only epidemics 4 and 5 correspond to a finite spatial range  $\kappa$ . For epidemics 2, 3, 6 and 8–10, the estimation yielded values for the cutoff parameter  $\kappa$  that were much larger than the spatial extent of the datasets and that were not converging to a clear best-fit value in our numerical optimization (which was carried out including the ‘FindMinimum’ function in Mathematica 10.0 and higher<sup>35</sup>), indicating that super-diffusive behavior extends across all length scales in the dataset. Therefore, for these epidemics, in the final ML estimation procedure we set the factor  $\exp(-\frac{r}{\kappa})$  equal to 1 (corresponding to assuming  $\kappa = \infty$ ) to remove the convergence problems. For the epidemics 1–5 (i.e. the epidemics without movement ban) the estimate of the scaling exponent  $\alpha$  ranges between 0.66 to 1.83 (with the majority of values between 1.45 and 1.83) and for the epidemics 6–11 (with movement ban) it ranges between 2.36 and 2.68; i.e. we observe a perfect separation of the parameter ranges between epidemics with and without movement ban. The AIC and the AIC<sub>0</sub> are significantly different (difference > 2) only for epidemics 4 and 5 (truncated Lévy-walk kernel performing better than the reference kernel). For the kernel estimation results taken from the literature (epidemics 1, 7 and 11), that literature gives results for non-truncated Lévy-flight kernels; i.e. no estimates for  $\kappa$  are available. The characteristic distance  $r_0$  ranges between 0.18 km and 2.7 km, i.e. spanning roughly one order of magnitude across the different epidemics. Differences in  $r_0$  are immaterial to the long-distance shape of the kernel as the latter is fully determined by the parameters  $\alpha$  and  $\kappa$ ; we note that this is illustrated by Fig. S1 where the graphs of the kernels for the epidemics 1–3 ( $\kappa = \infty$  and  $\alpha$  between 1.45 and 1.83) have very similar long-distance shapes and the same is observed for those of epidemics 6–11 ( $\kappa = \infty$  and  $\alpha$  between 2.36 and 2.68), and the graphs for the kernels of epidemics 4 and 5 each have a long-distance shape different from all other graphs due to a unique and finite value for  $\kappa$ . As the kernel amplitude  $\lambda_0$  does not inform about the distance dependence of transmission, we only report its estimated values in Table S1 for completeness.

In Fig. 1 we show the dendrogram result from the hierarchical clustering analysis of the value pairs  $\{\alpha, \kappa\}$  for the all 11 epidemics. This dendrogram indicates two main clusters, labelled 1 and 2, in which cluster 1 could be subdivided in two sub-clusters 1a and 1b. The clusters coincide completely with the grouping according to strategy ( $p < 0.001$ ): The epidemics 1–3 with strategy NMNZ are all located in cluster 1a, the epidemics 6–11 with strategy M are all located in cluster 1b, and the epidemics 4 and 5 with strategy NMZ are both located in cluster 2.

Nr	Strategy	$r_0$ (km)	$\alpha$	$\kappa$ (km)	AIC	AIC <sub>0</sub>
1	NMNZ	0.69 (0.41, 1.07)	1.72 (1.54, 1.93)	N/A	N/A	N/A
2	NMNZ	0.36 (0.02, 1.64)	1.83 (1.45, 2.39)	$\infty$	437.5	436.632
3	NMNZ	2.5 (0.48, 11.1)	1.45 (1.1, 2.1)	$\infty$	699.47	698.566
4	NMZ	1.32 (0.28, 3.44)	1.70 (1.39, 2.09)	173 (90, 932)	24,125.3	24,130.8
5	NMZ	0.18 (0, 18.7)	0.66 (0.38, 2.13)	25.3 (20.3, 45.9)	16,767.9	16,795.5
6	M	0.64 (0.43, 0.96)	2.56 (2.36, 2.82)	$\infty$	6800.09	6801.96
7	M	1.33 (1.1, 1.56)	2.68 (2.58, 2.78)	N/A	N/A	N/A
8	M	0.76 (0.17, 2.64)	2.36 (1.86, 3.21)	$\infty$	505.884	505.015
9	M	2.7 (1.2, 6.1)	2.53 (2.03, 3.46)	$\infty$	3089.80	3090.99
10	M	0.78 (0.003, 4.05)	2.47 (1.75, 3.98)	$\infty$	206.852	205.017
11	M	0.58	2.47	N/A	2093.08	2094.32

**Table 3.** Estimations for the 11 epidemics of the Lévy-walk kernel parameters  $r_0$ ,  $\alpha$  and  $\kappa$  (with confidence bounds between brackets), the corresponding AIC, the AIC<sub>0</sub> for the reference kernel estimation, and the applied control strategy (in order of increasingly stringent measures: no movement ban nor zoning (NMNZ), no movement ban but zoning (NMZ), and a movement ban (M)). For the kernel parameters of the transmission kernel for FMD in Japan (epidemic 11) no confidence bounds were reported in<sup>27</sup>.

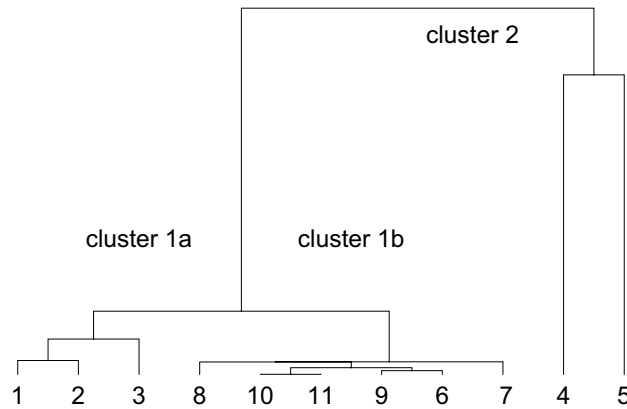


**Figure 1.** Dendrogram of the hierarchical clustering of the value pairs  $\{\alpha, \kappa\}$  for the 11 epidemics; two main clusters 1 and 2 are indicated, and within cluster 1 the two (sub)clusters 1a and 1b could be distinguished.

## Discussion

We gathered transmission kernel parameter estimates for 11 livestock disease epidemic datasets that together cover a broad range of host–pathogen combinations as well as combinations of control measures applied. A subsequent hierarchical clustering analysis of the parameter value combinations showed a maximal correlation between clusters and a grouping according to control measures. In particular, we observed a full separation of the ranges of estimates for the scaling exponent  $\alpha$  between strategies with movement ban (epidemics 6–11, coinciding with cluster 1b, where  $\alpha$  ranges between 2.36 and 2.68) and without movement ban (epidemics 1–5, coinciding with clusters 1a + 2, where  $\alpha$  ranges between 0.66 and 1.83). We observed that for the strategies without movement bans the scaling exponent is most often close to (and never significantly different from) the universal value of approximately 1.6 identified in analyses of human travel mobility patterns. This suggests that in absence of movement bans, the distance dependence of between-farm transmission is strongly determined by the pattern of between-farm animal transports; and that this pattern is characterized by a scaling exponent taking a value close to the universal value for human mobility. Indeed, modelling suggests that the power-law scaling of movements of infected individuals would be directly reflected in the spatial transmission pattern<sup>36</sup>. In line with this interpretation, we observe that only for the two epidemics with zoning measure (NMZ), the inclusion of the cutoff parameter  $\kappa$  leads to a better fitting model, suggesting that the zoning measure restricts the universal power-law dependence to distances in the order of the size of the zone. The applied protection zone of the 2006 BT epidemic in Germany (epidemic 11) was about 20 km and if zones overlapped they were merged to one larger zone<sup>11</sup>. The estimate for the cutoff distance  $\kappa$  epidemic 5 is 25.3 (20.3,45.9) km which we deem fully consistent with these zoning measures. The estimate for the cutoff distance in the 2006 BT epidemic in Belgium (epidemic 4) is 173 (90,932) km; as in this analysis (in contrast to the previous analysis reported in<sup>11</sup>) the populations of the Netherlands and France were also included, this 173 km represents an informative distance. This estimate is consistent with Belgium being declared one protection zone with the ‘radius’ of the country being about 140 km. The close correspondence, in both cases 4 and 5, between zoning measure and kernel shape further underpins the interpretation that constraining animal transports to within defined zones limits the dominant transmission route to distances within the extent of the zone. We note that although the analyses of the epidemics 1–3 and 6–11 do not produce a finite cutoff parameter, this is still consistent with the expectation that imposed export bans did produce a zoning effect on the scale of the country in question, as such an effect is not identifiable in an analysis including only the farm population within that country. Although the truncated Lévy-walk kernel is performing only better for epidemics 4 and 5 and similar for the other epidemics, the use of the truncated Lévy-walk kernel enables the comparison of the parameters of the different transmission kernels yielding further insight.

As noted above, for the six epidemics with movement bans the estimated scaling exponent ranges between 2.36 and 2.68 which is clearly different from the range (0.66–1.83) estimated for the 5 epidemics without movement ban, the difference being of the order of 1.0. The fact that the imposition of a movement ban produces such a dramatic shift of  $\alpha$ , implies that in absence of a movement ban, the longer-distance disease transmission is mainly driven by animal transports. Other possible transmission routes, such as human and fomite movements unrelated to animal transports, movements of wild animals and wind-borne virus dispersal, together may only play a minor role in the longer-distance disease transmission as long as no movement ban is in place. After imposition of a movement ban these other possible transmission routes are the ones remaining, and are yielding a scaling exponent that, compared to the situation without movement ban, seems to be increased by an amount of the order of 1.0. This difference of about 1.0 can be interpreted if we make two assumptions. First, we assume that the dispersal or movements underlying the remaining transmission routes are occurring predominantly in random directions, i.e. unlike animal transports these are not necessarily directed towards a neighboring farm. Second, we assume that these dispersal or movement processes are also described by a scaling exponent of approximately 1.6. The difference of about 1.0, which corresponds to a factor  $1/r$ , can then be explained from taking into account that for transmission to occur, the random movement direction of the infectious material has to match the direction towards a specific susceptible farm; the probability that this match occurs is inversely

proportional to the distance  $r$  to the susceptible farm<sup>36</sup>. Regarding the first assumption, we note that the indirect between-farm contacts occurring when e.g. feed delivery or egg collection trucks visit multiple farms on the same day, are clearly directed to the farms as destinations. I.e. these types of contacts do not correspond to movement with a random direction. This means that our assumption corresponds to a situation where only a minor part of infections can be attributed to these types of contacts, as was the case for epidemic number 9<sup>37</sup>. Regarding the second assumption, transmission via human movement, e.g. the route of a passerby accidentally connecting two farms, fits well into this interpretation as, Lévy-walk patterns with a scaling exponent of 1.6 have been identified for human movement<sup>23</sup>. This interpretation would thus support the hypothesis that ‘random’ human movement is the most important between-farm transmission route once animal movement bans are in place. However, the value of 1.6 does not exclusively point towards human movement. Concerning movement of wild animals, it is known of some species that they also move according a Lévy-walk pattern with a scaling exponent of about 1.6<sup>38</sup>. Concerning wind, specific atmospheric conditions can lead to aerial dispersal following a Lévy-walk pattern with a scaling exponent of about 1.5<sup>39</sup>. In addition, we note that our interpretation also implicitly assumes that the movement of infectious material between farms is fast enough such that pathogen survival is not influencing the scaling of transmission with distance.

Our results show that after imposing a movement ban, transmission retains its super-diffusive character, although the movement ban does reduce the longer-distance transmission risks by increasing the scaling exponent  $\alpha$  from around 1.6 to around 2.6. As long as transmission has a super-diffusive character (power-law dependence on distance), it will be difficult to spatially confine it using local control measures such as ring culling or ring vaccination.

The analyses in this paper provide a conceptual framework for analysis of spatial livestock disease spread and control. In addition to its relevance for interpreting past epidemic patterns and underpinning model extrapolations from these patterns, our approach provides a framework for assessing the spatial transmission of emerging livestock diseases, i.e. diseases for which no previous epidemic is available to estimate kernel parameters. As a prior model, the between-farm transmission could be assumed to follow a Lévy-walk kernel with parameter values as follows. The exponential power  $\alpha$  would be assumed to be about 2.6 if a movement ban is put in place and 1.6 without a movement ban. The spatial limitation  $\kappa$  would be assumed to equal the radius of the protection zone in case no movement ban is implemented and the radius of (a circular area approximating) the country when import bans are imposed by neighboring countries. According to Table 3, the characteristic distance  $r_0$  seems to be of the order of 1 km across all epidemics included. The remaining information needed for the Lévy-walk kernel, namely the value of the (relative) amplitude of the between-farm transmission ( $\lambda_0$ ) for the emerging disease in question, could be treated as a scenario parameter, to be varied within a plausible range. The resulting prior model can be used for analyses that can comprise risk maps for the spread of the emerging disease as well as more detailed evaluation of control measures by means of kernel model simulations<sup>6,9</sup>.

## Data availability

All data generated and analyzed during this study are included in this published article and its Supplementary Information file.

Received: 16 February 2022; Accepted: 20 February 2023

Published online: 02 March 2023

## References

- McElwain, T. F. & Thumbi, S. M. Animal pathogens and their impact on animal health, the economy, food security, food safety and public health. *Revue Scientifique Et Technique-Office International Des Epizooties* **36**, 423–433. <https://doi.org/10.20506/rst.36.2.2663> (2017).
- Saatkamp, H. W., Mourits, M. C. M. & Howe, K. S. A framework for categorization of the economic impacts of outbreaks of highly contagious livestock diseases. *Transbound. Emerg. Dis.* **63**, 422–434. <https://doi.org/10.1111/tbed.12286> (2016).
- Kao, R. R. The role of mathematical modelling in the control of the 2001 FMD epidemic in the UK. *Trends Microbiol.* **10**, 279–286 (2002).
- Matthews, L. *et al.* Neighbourhood control policies and the spread of infectious diseases. *Proc. R. Soc. B-Biol. Sci.* **270**, 1659–1666. <https://doi.org/10.1098/rspb.2003.2429> (2003).
- Ferguson, N. M., Donnelly, C. A. & Anderson, R. M. The foot -and-mouth epidemic in Great Britain: Pattern of spread and impact of interventions. *Science* **292**, 1155–1160 (2001).
- Boender, G. J. *et al.* Risk maps for the spread of highly pathogenic avian influenza in poultry. *PLoS Comput. Biol.* **3**, e71 (2007).
- Tildesley, M. J. & Keeling, M. J. Is  $R(0)$  a good predictor of final epidemic size: Foot-and-mouth disease in the UK (vol 258, pg 623, 2009). *J. Theor. Biol.* **259**, 863–863. <https://doi.org/10.1016/j.jtbi.2009.05.015> (2009).
- Boender, G. J., van Roermund, H. J. W., de Jong, M. C. M. & Hagenaars, T. J. Transmission risks and control of foot-and-mouth disease in The Netherlands: spatial patterns. *Epidemics* **2**, 36–47. <https://doi.org/10.1016/j.epidem.2010.03.001> (2010).
- Backer, J. A., van Roermund, H. J. W., Fischer, E. A. J., van Asseldonk, M. A. P. M. & Bergevoet, R. H. M. Controlling highly pathogenic avian influenza outbreaks: An epidemiological and economic model analysis. *Prev. Vet. Med.* **121**, 142–150. <https://doi.org/10.1016/j.prevetmed.2015.06.006> (2015).
- Chis Ster, I. & Ferguson, N. M. Transmission parameters of the 2001 Foot and mouth epidemic in Great Britain. *PLoS ONE* **2**, 1. <https://doi.org/10.1371/journal.pone.0000502> (2007).
- de Koeijer, A. A. *et al.* Quantitative analysis of transmission parameters for bluetongue virus serotype 8 in Western Europe in 2006. *Vet Res* **42**, 53. <https://doi.org/10.1186/1297-9716-42-53> (2011).
- Nassuato, C. *et al.* Spatial transmission of Swine Vesicular Disease virus in the 2006–2007 epidemic in Lombardy. *PLoS ONE* **8**, e62878. <https://doi.org/10.1371/journal.pone.0062878> (2013).
- Nathan, R., Klein, E. K., Robledo-Arnuncio, J. J. & E., R. Dispersal Kernels: Review. in *Dispersal Ecology and Evolution* (eds J. Clobert, M. Baguette, T. G. Benton, & J.M. Bullock) Ch. 15, 187–210 (Oxford University Press, 2012).
- Barbosa, H. *et al.* Human mobility: Models and applications. *Phys. Rep.* **734**, 1–74. <https://doi.org/10.1016/j.physrep.2018.01.001> (2018).
- Kot, M., Lewis, M. A. & van den Driessche, P. Dispersal data and the spread of invading organisms. *Ecology* **77**, 2027–2042 (1996).

16. van Saarloos, W. Front propagation into unstable states. *Phys. Rep.* **386**, 29–222 (2003).
17. Brockmann, D., Hufnagel, L. & Giesel, T. The scaling laws of human travel. *Nature* **439**, 462–465 (2006).
18. Lewis, M. A. & Pacala, S. Modeling and analysis of stochastic invasion processes. *J. Math. Biol.* **41**, 387–429 (2000).
19. Zhao, K. & Jurdak, R. Understanding the spatiotemporal pattern of grazing cattle movement. *Sci. Rep.* **6**, 31967. <https://doi.org/10.1038/srep31967> (2016).
20. Ramos-Fernandez, G. *et al.* Levy walk patterns in the foraging movements of spider monkeys (*Ateles geoffroyi*). *Behav. Ecol. Sociobiol.* **55**, 223–230. <https://doi.org/10.1007/s00265-003-0700-6> (2004).
21. Reynolds, A. M. *et al.* Displaced honey bees perform optimal scale-free search flights. *Ecology* **88**, 1955–1961. <https://doi.org/10.1890/06-1916.1> (2007).
22. Sims, D. W. *et al.* Scaling laws of marine predator search behaviour. *Nature* **451**, 1098–U1095. <https://doi.org/10.1038/nature06518> (2008).
23. Gonzalez, M. C., Hidalgo, C. A. & Barabasi, A.-L. Understanding individual human mobility patterns. *Nature* **453**, 779–782 (2008).
24. Rhee, I. *et al.* On the Levy-Walk nature of human mobility. *Ieee ACM Trans. Network* **19**, 630–643. <https://doi.org/10.1109/Tnet.2011.2120618> (2011).
25. Maruyama, Y. & Murakami, J. Truncated Levy walk of a nanocluster bound weakly to an atomically flat surface: Crossover from superdiffusion to normal diffusion. *Phys. Rev. B* **67**, 1. <https://doi.org/10.1103/Physrevb.67.085406> (2003).
26. Ming, Z., Mason, L. & Wenye, W. Empirical study on human mobility for mobile wireless networks. in *Military Communications Conference, 2008. MILCOM 2008. IEEE.* 1–7.
27. Hayama, Y., Yamamoto, T., Kobayashi, S., Muroga, N. & Tsutsui, T. Mathematical model of the 2010 foot-and-mouth disease epidemic in Japan and evaluation of control measures. *Prev. Vet. Med.* **112**, 183–193. <https://doi.org/10.1016/j.prevetmed.2013.08.010> (2013).
28. Koeijer, A. A., Hagenaars, T. J., Leuken, J., Swart, A. N. & Boender, G. J. (2020) Spatial transmission risk during the 2007–2010 Q fever epidemic in The Netherlands: Analysis of the farm-to-farm and farm-to-resident transmission. *PLoS One* **15**, e0227491. <https://doi.org/10.1371/journal.pone.0227491>.
29. Boender, G. J., van den Hengel, R., van Roermund, H. J. W. & Hagenaars, T. J. (2014) The Influence of Between-Farm Distance and Farm Size on the Spread of Classical Swine Fever during the 1997–1998 Epidemic in The Netherlands. *PLoS One* **9**, e95278. <https://doi.org/10.1371/journal.pone.0095278>.
30. Ferguson, C. E., Donnelly, C. A. & Anderson, R. M. Transmission intensity and impact of control policies on the foot and mouth epidemic in Great Britain. *Nature* **413**, 542–548 (2001).
31. Boender, G. J. *et al.* (2014) Confirmation of spatial patterns and temperature effects in Bluetongue virus serotype-8 transmission in NW-Europe from the 2007 reported case data. *Vet. Res.* **45**, Art 75. <https://doi.org/10.1186/S13567-014-0075-X>.
32. Akaike, H. (1974) New Look at Statistical-Model Identification. *IEEE Trans. Automat. Contr.* **Ac19**, 716–723. <https://doi.org/10.1109/Tac.1974.1100705>.
33. Burnham, K. P. & Anderson, D. R. *Model selection and multimodel inference: A practical information-theoretic approach.* (Springer, 2002).
34. Wolfram Research. *DendrogramPlot*, <<https://reference.wolfram.com/language/HierarchicalClustering/ref/DendrogramPlot.html>> (2007).
35. Wolfram Research. *FindMinimum*, <<https://reference.wolfram.com/language/ref/FindMinimum.html>> (2014).
36. Brockmann, D. Human Mobility and Spatial Disease Dynamics. in *Reviews of Nonlinear Dynamics and Complexity* (ed H.G. Schulster) 1–24 (Wiley-VCH, 2009).
37. Ssematimba, A., Elbers, A. R., Hagenaars, T. J. & de Jong, M. C. (2012) Estimating the per-contact probability of infection by highly pathogenic avian influenza (H7N7) virus during the 2003 epidemic in The Netherlands. *PLoS One* **7**, e40929. <https://doi.org/10.1371/journal.pone.0040929>.
38. Martins, M. L. *et al.* Cellular automata model for citrus variegated chlorosis. *Phys. Rev. E Stat. Phys. Plasmas, Fluids, Rel. Interdiscipl. Top.* **62**, 7024–7030. <https://doi.org/10.1103/physreve.62.7024> (2000).
39. Reynolds, A. M. Beating the odds in the aerial lottery: Passive dispersers select conditions at takeoff that maximize their expected fitness on landing. *Am. Nat.* **181**, 555–561. <https://doi.org/10.1086/669677> (2013).
40. Bellini, S., Alborali, L., Zanardi, G., Bonazza, V. & Brocchi, E. Swine vesicular disease in northern Italy: diffusion through densely populated pig areas. *Rev. Sci. Tech. Oie* **29**, 639–648. <https://doi.org/10.20506/rst.29.3.2006> (2010).
41. Elbers, A. R. W. *et al.* Field observations during the Bluetongue serotype 8 epidemic in 2006 - II. Morbidity and mortality rate, case fatality and clinical recovery in sheep and cattle in the Netherlands. *Prev. Vet. Med.* **87**, 31–40. <https://doi.org/10.1016/j.prevetmed.2008.06.003> (2008).
42. Méroc, E. *et al.* Establishing the spread of bluetongue virus at the end of the 2006 epidemic in Belgium. *Vet. Microbiol.* **131**, 133–144. <https://doi.org/10.1016/j.vetmic.2008.03.012> (2008).
43. Conraths, F. J. *et al.* Epidemiology of Bluetongue Virus Serotype 8, Germany. *Emerg. Infect. Dis.* **15**, 433–435. <https://doi.org/10.3201/eid1503.081210> (2009).
44. Bouma, A. *et al.* The foot-and mouth disease epidemic in The Netherlands in 2001. *Prev. Vet. Med.* **57**, 155–166 (2003).

## Acknowledgements

This project was funded by the Dutch Ministry of Agriculture, Nature and Food Quality (LNV), project code WOT-01-003-100.

## Author contributions

Both authors wrote and reviewed the main manuscript. G.J.B. performed the data analysis and visualized results in the figure. Both authors contributed to the interpretation and conceptualization.

## Competing interests

The authors declare no competing interests.

## Additional information

**Supplementary Information** The online version contains supplementary material available at <https://doi.org/10.1038/s41598-023-30230-w>.

**Correspondence** and requests for materials should be addressed to G.J.B.

**Reprints and permissions information** is available at [www.nature.com/reprints](http://www.nature.com/reprints).

**Publisher's note** Springer Nature remains neutral with regard to jurisdictional claims in published maps and institutional affiliations.



**Open Access** This article is licensed under a Creative Commons Attribution 4.0 International License, which permits use, sharing, adaptation, distribution and reproduction in any medium or format, as long as you give appropriate credit to the original author(s) and the source, provide a link to the Creative Commons licence, and indicate if changes were made. The images or other third party material in this article are included in the article's Creative Commons licence, unless indicated otherwise in a credit line to the material. If material is not included in the article's Creative Commons licence and your intended use is not permitted by statutory regulation or exceeds the permitted use, you will need to obtain permission directly from the copyright holder. To view a copy of this licence, visit <http://creativecommons.org/licenses/by/4.0/>.

© The Author(s) 2023